

Relationship Between Molecular Structure and Thermo-mechanical Properties of Candelilla Wax and Amides Derived from (*R*)-12-Hydroxystearic Acid as Gelators of Safflower Oil

Jorge F. Toro-Vazquez · Juan Morales-Rueda ·
V. Ajay Mallia · Richard G. Weiss

© Springer Science+Business Media, LLC 2010

Abstract In this research, we studied the relationship between the molecular structure of (*R*)-12-hydroxyoctadecanamide, (*R*)-*N*-propyl-12-hydroxyoctadecanamide, and (*R*)-*N*-octadecyl-12-hydroxyoctadecanamide and the thermo-mechanical properties of their 2% (wt/wt) organogels developed using safflower oil high in oleic acid (HOSFO) as the liquid phase. Candelilla wax (CW), a well-known edible gelling additive whose main component is hentriacontane, also was studied for comparative purposes. The results obtained show that the attractive interactions (i.e., hydrogen bonding and dipolar interactions) between amide groups and between hydroxyl groups present in the amides resulted in organogels with higher melting temperature, heat of melting, and crystallization parameters than those found in the CW organogel. The rheological parameters associated to the strength of the amide or CW-based gels developed in HOSFO (i.e., yield stress and elastic modulus) seem to be associated with the nature of amide groups (i.e., primary or secondary amide) and the increase in the length of the self-assembly molecular unit (i.e., *L* value determined by X-ray diffraction) and therefore to the extent

of London dispersion forces along the hydrocarbon chain. The creep and recovery measurements allowed an evaluation among the internal structures of the different organogels and demonstrated that independent of the hydrogen bonding and dipolar interaction provided by the amide and the hydroxyl groups, the increase in the hydrocarbon chain length results in higher organogel resistance to deformation and higher instant recovery capacity. However, the stabilization of the self-assembly unit through polar groups (i.e., –CONH₂ in HOA) reduces organogel elasticity but provides a higher extended recovery capacity. The results reported in this investigation showed some relationships between gelator structure and the thermo-mechanical properties of low-molecular-mass organic gelator amides. Our long-term objective is to understand the organogelation process to eventually develop *trans*-free vegetable oil-based food products with novel textures for the consumers.

Keywords Organogels · Hydroxystearic acid · Candelilla wax · Thixotropy · Creep and compliance

J. F. Toro-Vazquez · J. Morales-Rueda
Facultad de Ciencias Químicas-CIEP,
Universidad Autónoma de San Luis Potosí,
San Luis Potosí SLP 78210, México

V. A. Mallia · R. G. Weiss
Department of Chemistry, Georgetown University,
Washington, DC 20057-122, USA

J. F. Toro-Vazquez (✉)
Facultad de Ciencias Químicas-CIEP, Zona Universitaria,
Av. Dr. Manuel Nava 6,
San Luis Potosí SLP 78210, México
e-mail: toro@uaslp.mx

Introduction

Molecular organogels are bi-continuous, frequently colloidal systems that coexist as aggregated gelator molecules and an organic liquid. In general, organogel formation is based on the spontaneous self-assembly of individual gelator molecules into three-dimensional networks of randomly entangled fiber-like or plate-like structures. This three-dimensional network holds microdomains of the liquid in a non-flowing state mainly through surface tension and capillary forces.¹ In these systems, the gelator is a low-molecular-mass organic molecule (LMOG) which is only slightly soluble in the

liquid at the temperatures where the gel exists (most commonly at room temperature and above). Examples include apolar and amphiphatic molecules such as cholesteryl anthraquinone derivatives,² sterols,³ lecithin,⁴ sorbitan monostearate,⁵ *n*-alkanes,^{1,6} and (*R*)-12-hydroxystearic acid (i.e., (*R*)-12-hydroxyoctadecanoic acid).⁷ The latter is a well-known gelator of organic liquids commonly used in deodorant sticks, antiperspirant gels, and as a surfactant cleansing agent in several cosmetic products. Aggregation of LMOGs occurs primarily through van der Waals forces, specific intermolecular hydrogen bonding, electrostatic forces, π - π stacking, or even London dispersion forces.⁸ The nature of both the solvent and the LMOG determine which intermolecular forces predominate to stabilize the self-assembled primary structure, the growth mode, and, subsequently, the organogel microstructure and thermo-mechanical properties.

However, the relationship between gelator chemical structure and its gelling capability is not evident a priori in most cases.^{9,10} Therefore, a great deal of further investigation is needed to discover the factors that establish suitable gelator–solvent combinations with specific functional properties for particular applications. Mallia et al.⁸ studied the relationship between molecular structure and the gelation properties of LMOG amides and amines based on (*R*)-12-hydroxystearic acid in several organic liquids. These LMOG amides and amines were constructed to differ structurally in a rational way so that some chemical structure–physical property relationships could be established.⁸ Thus, the presence of a primary amide group in one of these LMOGs instead of the carboxylic group of hydroxystearic acid increases gelator efficiency. However, the primary amine analog is less efficient than the parent acid. Additionally, some of the organogels with the *N*-containing derivatives of (*R*)-12-hydroxystearic acid, especially those with amide functionalities, exhibited thixotropic behavior. However, the kinetics of recovery of these mechanically destroyed gels was too fast to be measured properly by the rheological technique employed, and the results may have been affected by slippage between the rheometer plates and the sample.⁸

Thus, a primary aim of this study was to determine the relationship between the molecular structure of LMOG amides and the thermo-mechanical properties of their organogels using safflower oil high in oleic acid as the liquid phase. We have given careful attention to the determination of the organogels' thixotropic behavior, evaluated as creep and recovery profiles.

The LMOG amides used in this investigation were (*R*)-12-hydroxyoctadecanamide (HOA), (*R*)-*N*-propyl-12-hydroxyoctadecanamide (P-HOA), and (*R*)-*N*-octadecyl-12-hydroxyoctadecanamide (O-HOA; Figure 1), synthesized from (*R*)-12-hydroxystearic acid. These amides can be viewed as *n*-alkanes of different lengths with a hydroxyl

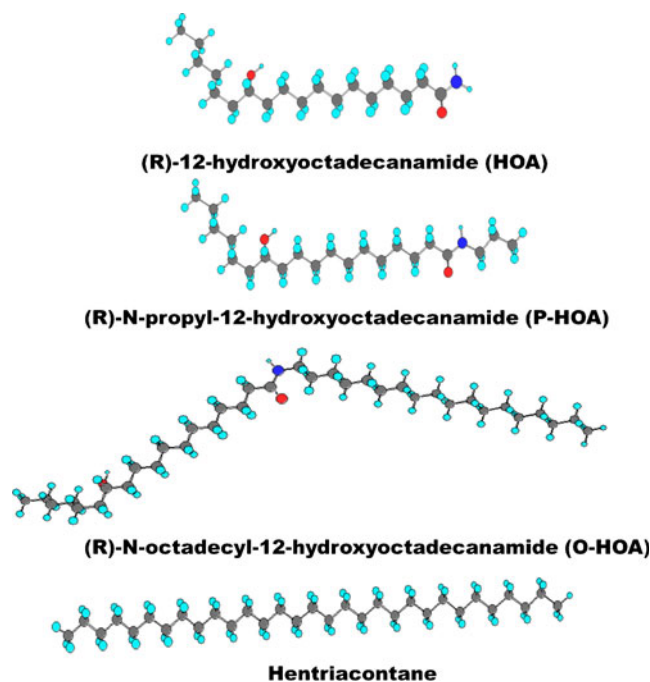


Fig. 1 Structures of the LMOG amides investigated. Hentriacontane is the main component in CW. The structures were made using CS Chem3D Ultra Molecular Modeling and Analysis Cambridgesoft, Cambridge, MA. V. 7.0.0 (2001)

substituent at carbon-12 and an amide functionality placed either at a chain terminus or inserted along the chain. Thus, the results obtained with these LMOG amides have been compared with those from safflower oil gels in which the LMOG is candelilla wax (CW) whose main component is a long *n*-alkane, hentriacontane ($\text{CH}_3(\text{CH}_2)_{29}\text{CH}_3$).^{11,12} Candelilla wax is a food additive recognized worldwide and approved by the FDA (under regulations 21CFR, 175.105, 175.320, 176.180). The 3% CW organogels developed in safflower oil¹¹ have shown a phase separation stability at room temperature at least up to 8 to 12 months, providing textures with potential use for the food industry.

Materials and Methods

Materials

The LMOG amides were prepared, purified, and characterized as described by Mallia et al.⁸ Safflower oil, high in triolein (HOSFO) and extracted from genetically modified seed, was obtained from Coral Internacional (San Luis Potosí, Mexico). Micron-powdered, high-purity CW was supplied by Multiceras (Monterrey, Mexico). HOSFO and CW were characterized previously by HPLC and capillary GC–mass spectrometry.^{11,12} CW contained 78.9% ($\pm 0.1\%$) hentriacontane as well as minor amounts of other alkanes such as nonacosane ($4.2 \pm 0.1\%$) and tritriacontane ($8.0 \pm$

0.2%) and 7.4% ($\pm 0.1\%$) of triterpene alcohol(s) with a molecular formula of $C_{30}H_{49}OH$ (i.e., germanicol, lupeol, or moretenol). The major triacylglycerol in HOSFO was triolein with 63.32% ($\pm 0.06\%$). Each LMOG amide or CW was solubilized in HOSFO by heating (140 °C) and agitation to obtain a 2% (wt/wt) solution.

Calorimetry of Neat LMOG Amides, CW, and Their 2% Gels in HOSFO

A differential scanning calorimeter, model Q1000 from TA Instruments (New Castle, Delaware, USA) was used for dynamic crystallization and melting studies. Samples of neat LMOG amides and CW ($\approx 5\text{--}7$ mg) were sealed in aluminum pans, heated at 140 °C for 20 min, and then cooled to -20 °C at 10 °C/min. After 2 min at -20 °C, the system was heated to 140 °C at 5 °C/min. For the 2% (wt/wt) gelator samples, $\approx 7\text{--}10$ mg was sealed in the aluminum pans and heated at 120 °C for 20 min, cooled to 10 °C (20 °C/min), maintained at this temperature for 5 min, and then heated to 25 °C (5 °C/min). After 75 min at this temperature, the samples were melted by heating to 120 °C (5 °C/min). The temperature at the beginning of the crystallization exotherm (T_g), the heat of crystallization (ΔH_g), the temperature at the peak of the melting endotherm (T_p), and the heat of melting (ΔH_M) were calculated with the instrument software (TA-Instruments Universal Analysis 2000, v. 4.2E). T_g and T_p were calculated from inflections in the first derivative of the heat flux. T_g was the temperature where the first derivative of the heat capacity of the sample initially departed from the baseline, and T_p was the temperature where the first derivative of the heat capacity associated with the melting endotherm returned to the baseline. ΔH_g and ΔH_M values correspond to the areas under the crystallization exotherm and melting endotherm, respectively. At least two independent determinations were done, and the mean and standard deviation were used for statistical analysis (STATISTICA V 9.0; StatSoft Inc., Tulsa, OK).

G'/G'' and Creep and Recovery Profiles

The elastic (G') and loss (G'') moduli of the organogels formed upon cooling 2% solutions were determined with a mechanical spectrometer (Paar Physica MCR 301, Stuttgart, Germany) using a steel cone-plate geometry (CP25-1/TG, Anton Paar, Graz, Austria) equipped with a true-gap system. This device makes the corrections in gap size associated with the expansion/shrinkage of the sample and/or the rheometer geometry due to changing temperature conditions used during measurements.¹³ Temperature was controlled by a Peltier system located in both the base and top of the measurement geometry through a Peltier-controlled hood (H-PTD 200). The control of the equipment was made through

the software Start Rheoplus US200/32, version 2.65 (Anton Paar). An aliquot of a 2% sample was placed on the base plate of the rheometer and the cone was set using the true-gap function of the software. The same time-temperature program as in the calorimetry studies was employed. Thus, after 10 min at 120 °C, the sample was cooled to 10 °C at 20 °C/min. After 5 min at this temperature, the sample was heated (5 °C/min) to 25 °C, and after 15 min, G' and G'' were measured during 60 min, always within the linear viscoelastic region (LVR). At the frequencies used (i.e., 0.5 or 1.0 Hz), the strain (γ) applied was always within 0.002% and 0.01%. After 75 min at 25 °C, the yield stress (σ^*) of the organogels was determined applying a strain sweep between 0% and 100%. σ^* was calculated from a log-log plot of shear stress vs. γ (%) at the corresponding upper limit of strain. To determine the creep and recovery profile, new organogel aliquots were employed using the same time-temperature conditions as before. After 75 min at 25 °C, a constant stress (i.e., 11.25 Pa) was applied to the gels for 60 s while measuring the γ (i.e., creep stage). After this time, the force was withdrawn while γ measurements continued for an additional 300 s (i.e., recovery stage). The creep (i.e., slow and progressive deformation of the material under constant stress) and recovery profiles were determined by plotting the compliance (J) as a function of time. J is the ratio between γ of the sample and the stress applied. The stress applied was selected based on σ^* profiles and exploratory creep and recovery measurements with the 2% organogels (*vide infra*). In all cases, two independent determinations were made and the mean used for statistical analysis.

Fitting the Creep and Recovery Profile

To investigate the relationship between the rheological properties of the organogels and the three-dimensional crystal network of the organogels, the creep profile was fitted to Burger's model (Eq. 1) and the recovery profile to Eq. 2.¹⁴ The corresponding parameters were obtained using the quasi-Newton methodology available in the nonlinear estimation procedure of STATISTICA V 9.0 (StatSoft Inc.). The percent recovery achieved at 60 and 300 s after releasing the stress was calculated using Eq. 3.

$$J(t) = \frac{1}{G_0} + \frac{1}{G_1} \left[1 - \exp\left(\frac{-tG_1}{n_1}\right) \right] + \frac{t}{n_0} \quad (1)$$

$$J = J_\infty + J_{KV} \exp(-Bt^C) \quad (2)$$

$$\text{Recovery \%} = \frac{J_{MAX} - J(t)}{J_{MAX}} \times 100 \quad (3)$$

$$J_{SM} = J_{MAX} - (J_\infty + J_{KV}) \quad (4)$$

In Eq. 1 (Figure 2a), G_0 is the instantaneous elastic modulus and defines the sample's resistance to deformation (i.e., G_0 occurs immediately during the deformation profile and is instantaneously recovered when the stress is removed), G_1 is the contribution of the retarded elastic region to the total compliance, n_0 is the residual viscosity or viscous flow of the system after suffering deformation, and n_1 is the internal viscosity. In Eq. 2 (Figure 2b), J_∞ corresponds to the permanent or residual deformation, J_{KV} is a slow or retarded recovery due to a decreasing exponential type and tends toward an asymptote when $t \rightarrow \infty$, B and C are parameters that define the recovery speed of the sample which can be calculated from the first derivative with respect to time for Eq. 2. The B and C parameters were not calculated in this investigation. The percentage of recovery achieved by the gel at a given time ($\%R_t$) was calculated with Eq. 3, where J_{MAX} is the maximum compliance achieved during the creep profile (Figure 2b) and $J(t)$ is the compliance at $t=60$ s or $t=300$ s

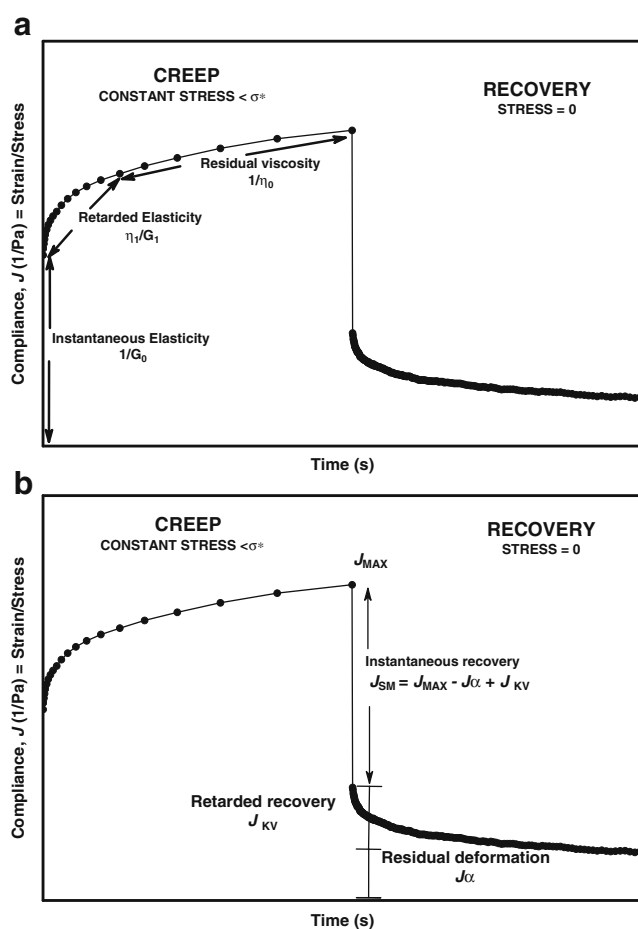


Fig. 2 Description of the Burger's parameters in a generalized creep (a) and recovery (b) profile. The parameters associated with Burger's equation (Eq. 1) and the ones calculated with Eqs. 2 and 3 are defined in the text

after the stress force was withdrawn. On the other hand, the initial or instantaneous shear compliance of the system, J_{SM} (Figure 2b), is difficult to determine experimentally and was calculated using Eq. 4, where J_∞ is the compliance at a given time ($t=60$ or 300 s).

X-Ray Analyses

Powder X-ray diffraction patterns of samples were obtained as described in ⁸ using a Rigaku R-Axis image plate system with CuK α R X-rays ($\lambda=1.54$ Å) generated by a Rigaku generator operating at 46 kV and 40 mA with the collimator at 0.5 mm. Data processing and analyses were performed using Materials Data JADE (version 5.0.35) XRD pattern processing software. The samples were sealed in 0.5-mm glass capillaries (W. Müller, Schönwalde, Germany), and diffraction data were collected for 2 h (neat powders) or 10 h (gels).

Polarized Light Microscopy

Polarized light microphotographs (PLM) of the organogels were obtained using a polarizing light microscope (Olympus BX51; Olympus Optical Co., Ltd., Tokyo, Japan) equipped with a color video camera (KP-D50; Hitachi Digital, Tokyo, Japan) and a heating/cooling stage (TP94; Linkam Scientific Instruments, Ltd., Surrey, England) connected to a temperature control station (LTS 350; Linkam Scientific Instruments, Ltd.) and a liquid nitrogen tank. A 100 μ L aliquot of a melted sample was dropped over a preheated glass microscope slide (≈ 120 °C). A glass cover was placed on the top and the same thermal treatment as for the calorimetry and rheological studies was applied using a temperature control station (Linksys32 V 1.3.1; Linkam Scientific Instruments Ltd., Waterfield, UK). PLMs of the organogels were obtained after they had been at 25 °C for 75 min.

Results and Discussion

Thermal Parameters for the Neat Gelators and the 2% Organogels

Overall, the strong hydrogen bonding (from complementary H-bond donating/accepting motifs) and dipolar interactions between amide groups and between hydroxyl groups of the LMOG amides results in higher temperatures and heats of melting (i.e., T_M and ΔH_M) and solidification (i.e., T_g and ΔH_g) parameters in both the neat gelators and their 2% organogels than those found for the corresponding samples with CW (Table 1). Similar results have been reported for gels of LMOG amides with silicone oil as the liquid.⁸ The intermolecular stabilizing forces in neat CW and its three-

Table 1 Thermal parameters (crystallization and melting) for neat gelators and for 2% (wt/wt) organogels in HOSFO

	Neat gelators				2% Organogels			
	T_g (°C)	ΔH_g (J/g)	T_M (°C)	ΔH_M (J/g)	T_g (°C)	ΔH_g (J/g)	T_M (°C)	ΔH_M (J/g)
HOA	109.69 ^a (0.25)	177.95 ^a (5.44)	113.70 ^a (0.81)	178.75 ^a (1.91)	93.27 ^a (3.33)	4.23 ^a (0.24)	100.35 ^a (1.25)	4.22 ^a (0.12)
P-HOA	99.99 ^b (0.06)	173.90 ^a (0.78)	106.93 ^b (0.01)	179.30 ^a (0.99)	73.26 ^b (3.15)	3.54 ^b (0.21)	90.58 ^b (0.39)	3.29 ^b (0.15)
O-HOA	102.75 ^c (0.28)	167.50 ^b (1.98)	106.74 ^b (0.01)	164.05 ^b (2.05)	76.85 ^b (0.42)	3.82 ^b (0.15)	88.70 ^c (1.20)	3.97 ^c (0.07)
CW	76.58 ^d (0.68)	147.35 ^c (1.91)	64.42 ^c (0.23)	149.75 ^c (1.20)	35.83 ^c (0.18)	1.26 ^c (0.03)	39.16 ^d (0.06)	2.50 ^d (0.21)

^{a, b, c, d}The same thermal parameter values with the same letter indicate no significant difference. Values with a different letter indicate a significant difference ($P < 0.10$)

dimensional gel network are principally weaker van der Waals dispersion forces; as mentioned, *n*-alkanes are the main components of CW. Another factor, the solubility of the LMOG amides, being lower than that of CW in the low polarity liquid HOSFO contributes to the greater stability of the amide-based gels. HOA has the highest crystallization and melting parameters of the three amides in both its neat state and at 2% in HOSFO. The molecular structure of HOA has one more hydrogen attached to the nitrogen atom than the secondary amides, P-HOA and O-HOA, and therefore can develop a more extensive H-bonding network within its gel fibers.

Rheological Behavior

The protocol for making the organogels for rheological studies followed those adopted previously.⁸ The G' profiles of the organogels at 25 °C during 60 min is shown in Figure 3. Overall, they are relatively constant over time (i.e., P-HOA and CW) or increased slightly with time and reached a plateau after 20–30 min (i.e., HOA and O-HOA). The relationship between G' of the organogels and the molecular structures of their gelators will be discussed later.

σ^* is defined in engineering and materials science as the stress at which a material begins to deform plastically. At forces lower than σ^* , a material deforms elastically and returns to its original shape when the applied stress is removed. Once forces higher than σ^* are applied, some fraction of the deformation will be permanent and non-reversible. The σ^* values of the 2% organogels after 60 min at 25 °C are reported in Table 2. The CW gel showed the lowest σ^* , followed by P-HOA, HOA, and O-HOA in increasing order ($P < 0.05$). As previously discussed, ΔH_M is a parameter directly associated with the intermolecular

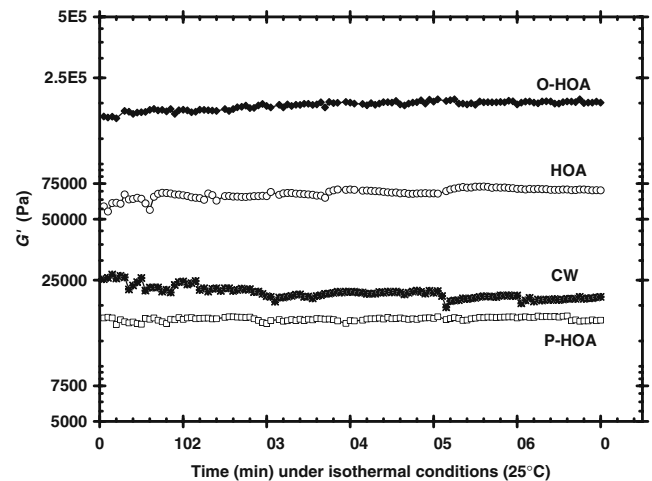


Fig. 3 G' profile as a function of time for the 2% organogels formed at 25 °C in HOSFO

Table 2 Yield stress (σ^*), mean G' , and Burger's parameters for the 2% organogels. The Burger's parameters were obtained by fitting the experimental creep profile to the Burger's equation

Gelator	Burger's parameters								
	σ^* (Pa)	G' (Pa) ^c $\times 10^4$	G_0 (Pa) $\times 10^4$	η_0 (Pa) $\times 10^6$	G_1 (Pa) $\times 10^5$	η_1 (Pa) $\times 10^5$	λ_{ret} (s)	R^{2f}	Mean square error ^g ($\times 10^{-13}$)
P-HOA	83.8 ^a (5.2)	1.62 ^a (0.03)	1.55	6.60	1.51	3.41	2.257	0.986	1.319
CW	22.5 ^b (9.1)	2.08 ^b (0.08)	3.39	6.47	1.17	3.55	3.023	0.991	2.921
HOA	175.5 ^c (34.6)	7.07 ^c (0.10)	6.35	22.26	2.13	11.00	5.160	0.979	3.934
O-HOA	189.0 ^c (28.3)	18.9 ^d (0.31)	8.66	10.28	1.92	5.71	2.972	0.991	2.543

a, b, c, d σ^* and G' values with the same letter indicate no significant difference. Values with a different letter indicate a significant difference ($P < 0.05$)

^c Mean calculated from G' values of the last 20 to 30 min of the G' profile

^f Determination coefficient of the model

^g Calculated as $\sum(\text{estimated value} - \text{experimental value})^2/n$, where n is the total number of data used to fit the equation

forces that stabilize the self-assembled primary structure of the gelator and, therefore, with the structural organization of the gelator molecules in their gel networks. Within this context, the σ^* of the organogels showed a linear relationship with ΔH_M [$\sigma^* = -230.07 + 99.5(\Delta H_M)$; $R^2 = 0.9474$, $P = 0.0267$]. Thus, the higher the ΔH_M , the higher the stress required to produce a permanent deformation in an organogel.

The stress applied to determine the creep and recovery profiles of the 2% organogels (i.e., 11.25 Pa, a force equivalent to $\approx 50\%$ the σ^* for the 2% CW organogel) was selected based on the σ^* profiles obtained for the 2% organogels and exploratory creep and recovery measurements. Excessive force produced a fast and high deformation with very small recovery; too little force resulted in limited deformation and practically the same creep and recovery profiles even between different types of organogels. Overall, the creep and recovery profiles show the same general behavior (Figure 4). Thus, the creep profiles of the 2% organogels after samples had been incubated at 25 °C for 75 min showed progressive deformation of the LMOG network under constant stress (i.e., 60 s at 11.25 Pa). Upon release of the stress, the strain of the samples exhibited an instantaneous recovery followed by a progressive decrease of deformation until attaining a constant, non-zero value (i.e., after deformation, the organogels never attained full recovery).

The determinations of G_0 , G_1 , n_0 , and n_1 (Table 2), by fitting of the recovery profile to Burger's equation Eq. 1, allowed an evaluation among the internal structures of the different organogels because the same mechanical model was used to associate the behavior of the organogel in response to deformation. Within this framework, the retardation time, λ_{ret} , is equal to n_1/G_1 , a value characteristic of each system. If the system is a Hookean solid (i.e., completely elastic), the λ_{ret} would be zero and the

maximum strain would be obtained immediately after the application of a constant stress. However, viscoelastic materials are characterized by a delay in achieving the maximum strain (i.e., the delay of the elasticity). This delay time is λ_{ret} (i.e., the rate at which the maximum strain is achieved by the system).¹⁴

Thus, considering that the same stress was applied to all gels investigated here, G' showed a significant exponential relationship with G_0 (Figure 5), with P-HOA observing the lowest resistance to instantaneous deformation (i.e., the P-HOA organogel had the softest texture) followed in increasing order of hardness by the CW gel, the HOA (primary amide) gel, and the O-HOA gel, which showed the hardest texture. The organogels of HOA and O-HOA also have the highest σ^* , indicating the high degree of structural order in their gelator networks. The PLM are also consistent with these results (Figure 6). Thus, the 2%

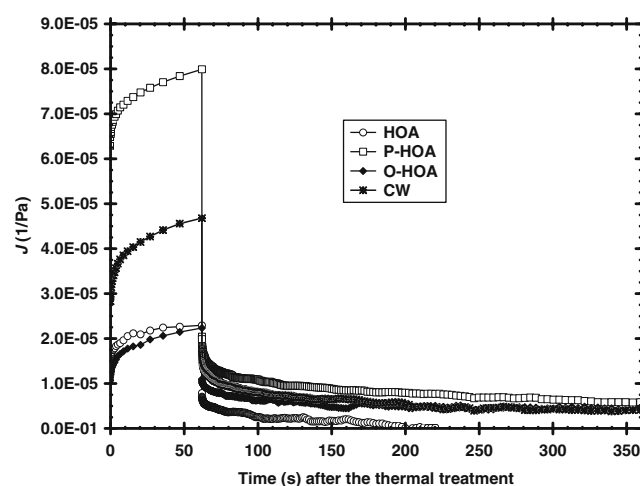


Fig. 4 Creep and recovery profile for the 2% organogels formed at 25 °C in HOSFO

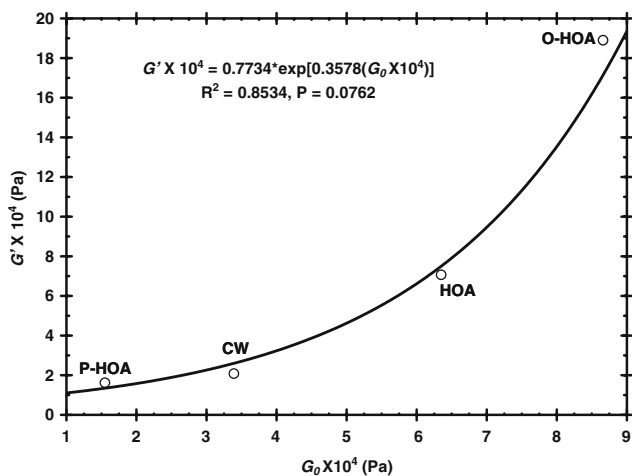


Fig. 5 Relationship between G' and G_0 of the 2% organogels. The fitting equation, the corresponding determination coefficient (R^2), and associated statistical significance (P) are shown

organogels of HOA (Figure 6a) and O-HOA (Figure 6c) exhibit larger spherulites with fibers that interweave to a higher extent than the spherulites developed by P-HOA gel (Figure 6b). In contrast, the microphotographs of the 2% CW organogel (Figure 6d) showed a three-dimensional network of interacting microplatelets, like that found previously for organogels with *n*-alkane gelators.¹⁵ As noted previously, the main component of CW is hentriacontane, an *n*-alkane with a chain length of 31 carbon atoms.^{11,12}

It is interesting to note that the exponential relationship between G' and G_0 (Figure 5) was also associated with the extended molecular lengths (L) calculated for the gelators

(i.e., amides and hentriacontane, taken to be representative of the molecular composition of CW). The L value is associated with the carbon number of the self-assembly molecular unit of the corresponding gelator. However, it is important to point out that such relationship considers that based on the packing arrangements of the gelator molecules determined from X-ray diffractograms (Table 3), the primary amide, HOA, develops stable H-bonding longitudinal interactions between opposing $-\text{CONH}_2$ groups of HOA molecules so that the actual repeat unit length is actually approximately twice the molecular length.¹⁴ O-HOA has a self-assembly length similar to that of HOA, but the long *N*-octadecyl chain of O-HOA (as well as the *N*-propyl chain of P-HOA) and limitations imposed on its H-bonding as a result of its secondary amide status results in having a single molecule repeat length. All of these results indicate that the higher G_0 (i.e., higher resistance to strain) and lower λ_{ret} (i.e., lower delay time as a result of higher elasticity) in the O-HOA organogel in contrast to the ones observed by HOA organogels are associated with the strength provided to the three-dimensional crystal network by the $-\text{CONH}-$ bond.

Thus, in a low-polarity liquid such as the HOSFO, the increase in the organogel resistance to deformation (Figure 5) seems to be associated with the increase in the length of the self-assembly molecular unit. However, for units of similar length (i.e., HOA and O-HOA), the stabilization of the self-assembly unit through polar groups (i.e., $-\text{CONH}_2$ in HOA) reduces organogel elasticity. This conclusion is based on the lower G_0 and higher λ_{ret} values observed in HOA than in O-HOA (Table 2). In the O-HOA organogel, the self-

Fig. 6 Polarized light microphotographs of 2% organogels formed at 25 °C in HOSFO. **a** 2% HOA; **b** 2% P-HOA; **c** 2% O-HOA; **d** 2% CW

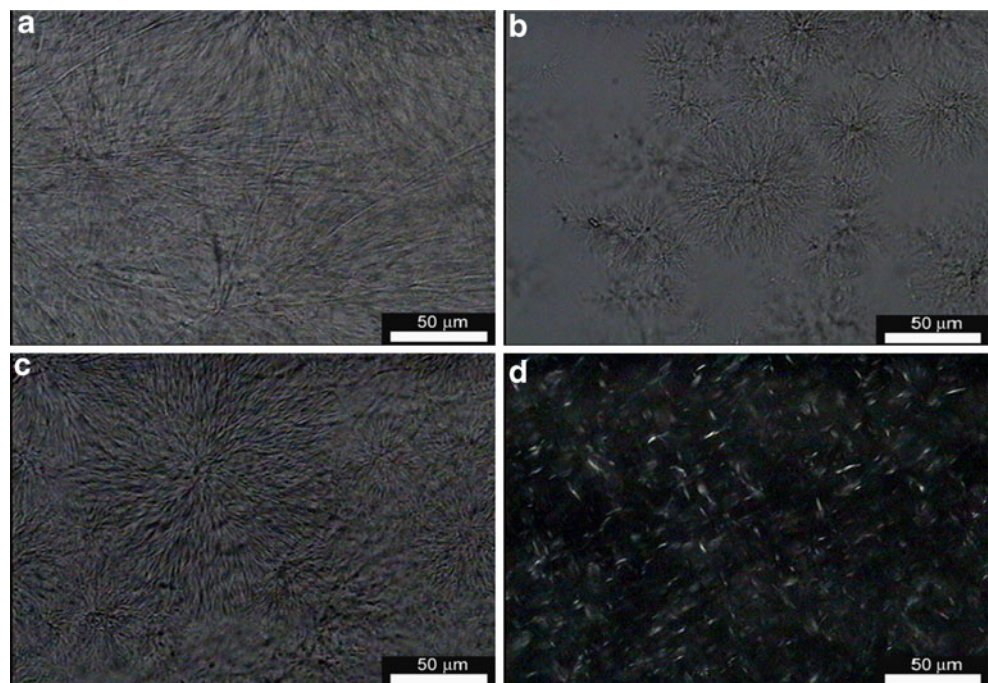


Table 3 Comparison of lattice spacings (d) and calculated extended molecular lengths (L) of HOA, P-HOA, O-HOA, and CW in neat powders and organogels (from XRD data at 22 °C)

Gelator	L^a (Å)	d (powder state, Å)	d (gel state, Å)	Probable packing arrangement in gel
HOA	26.4	48.5, 15.7, 4.5, 3.9, 3.8	48.5, 15.7, 4.5, 3.9, 3.8	Bilayer
P-HOA	31.1	28.5, 14.7, 10.8, 8.2, 4.7, 4.1, 3.9, 3.6	28.7, 14.2, 4.0	Monolayer
O-HOA	50.3	23.8, 16.0, 12.2, 9.5, 8.8, 4.6, 4.1, 3.9, 3.5	49.0, 15.9, 5.0, 4.4	Monolayer
CW	42.5 ^b	42.0, 20.9, 13.9, 8.2, 4.1, 3.9, 3.0, 2.5	28.6, 23.7, 14.7, 6.8, 5.8, 4.1, 3.7, 3.0, 2.5	Lamellar

^a Extended molecular lengths were calculated using Chem 3 D Ultra 8 software (Cambridge Soft Corporation, USA) and adding the van der Waals radii of the terminal atoms

^b Value for hentriacontane

assembly molecular unit retains many of the H-bonding characteristics of P-HOA, but the large number of London dispersive interactions along the *N*-octadecyl chains force molecules to align in layers of single molecular thickness. Thus, both the length of the hydrocarbon chain (i.e., London dispersion forces) and the nature of amide groups (i.e., van der Waals forces from the H-bonding interactions) determine the degree of elasticity, with the stabilization of the self-assembly unit through polar groups (i.e., $-\text{CONH}_2$) having the greater effect on the rheological properties.

The parameters that describe the recovery profile of the organogels at 60 and 300 s after releasing the stress are shown in Table 4. The instantaneous shear compliance (J_{SM}) and its corresponding contribution to the gel recovery ($\%R_{\text{SM}}$) are also shown in Table 4. The $\%R_{\text{SM}}$ was calculated using J_{SM} as J_{∞} in Eq. 3. According to Steffe,¹⁶ if samples under measurement follow the Burger model and the rheological measurements are made within the LVR, $1/G_0$ from the creep profile must be equal to J_{SM} in the recovery profile. Using the corresponding values reported in Tables 1 and 4, we can easily corroborate that this

condition is satisfied for all organogels investigated, and therefore, $\%R_{\text{SM}}$ provides a reliable measurement of the instantaneous recovery. J_{MAX} is the maximum compliance achieved during the creep profile, and therefore, it had an inverse relationship with G' and G_0 (Table 2). Both G' and G_0 are values directly associated with the organogel's resistance to deformation (i.e., the higher J_{MAX} , the lower the gel resistance to deformation).

After the stress was removed, the retarded recovery (J_{KV}) at 60 and 300 s was similar for HOA and O-HOA. However, O-HOA gels achieved a higher $\%R_{\text{SM}}$, but its recovery as a function of time was lower than in HOA gels (Table 4), a behavior associated with the higher resistance to deformation observed by O-HOA gels (compare G_0 values in Table 2). These results indicated that although O-HOA and HOA have a self-assembly unit with similar molecular length, the $-\text{CONH}-$ bond in O-HOA provides greater strength to the three-dimensional crystal network of the gel, higher $\%R_{\text{SM}}$, but limited retarded recovery capacity in comparison with HOA gels. In contrast, the stabilization of the self-assembly unit through polar groups

Table 4 J_{SM} , J_{∞} , J_{KV} , the instantaneous percentage of recovery ($\%R_{\text{SM}}$), and the percentage of recovery at $t=60$ s and $t=300$ s ($\%R_t$) for the 2% (wt/wt) organogels developed at 25 °C

Gelator	Time (t) s	J_{MAX} (1/Pa) $\times 10^{-5}$	J_{SM} (1/Pa) $\times 10^{-5}$	J_{∞} (1/Pa) $\times 10^{-5}$	J_{KV} (1/Pa) $\times 10^{-5}$	R^{2a}	Mean Square error ^b $\times 10^{-14}$	$\%R_{\text{SM}}$	$\%R_t$
HOA	60	2.30	1.55	2.84	3.59	0.9804	3.0948	32.6	90.4
	300			1.11	-0.36	0.9856	7.4065		107.3
P-HOA	60	7.99	5.77	6.25	8.40	0.9916	4.2551	27.8	88.1
	300			3.66	-1.38	0.9926	7.2354		92.7
O-HOA	60	2.24	1.02	2.50	3.70	0.9899	1.5887	54.5	72.8
	300			2.03	-0.72	0.9633	11.3989		79.2
CW	60	4.68	2.72	-69.4	-67.50	0.9911	4.7959	41.9	84.6
	300			3.45	-1.40	0.9862	13.6875		91.2

^a Determination coefficient of the model

^b Calculated as indicated in Table 2

in HOA (i.e., $-\text{CONH}_2$) provides softer gels with higher retarded recovery capacity but lower $\%R_{\text{SM}}$ in comparison with O-HOA gels.

P-HOA, also with a $-\text{CONH}-$ bond, developed gels with higher retarded recovery capacity but lower $\%R_{\text{SM}}$ than O-HOA gels. However, P-HOA gels had the softest texture of all gels evaluated (Table 2) and, therefore, the lower resistance to deformation (Figure 4). Thus, the increase in the length of the self-assembly molecular unit (i.e., number of London dispersive interactions along the hydrocarbon chain) seems to be associated with both the increase in the organogel resistance to deformation and the instant recovery capacity. This conclusion is supported by the higher G_0 and $\%R_{\text{SM}}$ observed by CW gels in contrast with the ones shown by P-HOA gels (Tables 2 and 4). Thus, the $\%R_{\text{SM}}$ showed a significant direct linear relationship with the calculated extended molecular lengths of the gelators (L value, Table 3) through the following equation:

$$\%R_{\text{SM}} = 1.35 + 1.01(L); R^2 = 0.863, P = 0.07.$$

In contrast, the percentage of recovery achieved by the amide organogels after 60 and 300 s ($\%R_t$) had an inverse linear relationship with L through the following equations:

$$\%R_{t=60\text{s}} = 109.3 - 0.67(L); R^2 = 0.8715, P = 0.066$$

$$\%R_{t=300\text{s}} = 129.02 - 0.97(L); R^2 = 0.833, P = 0.087.$$

These relationships seem to apply also to the CW organogel in spite of its gelator network (i.e., interlocking platelets) which is vastly different from those of the amide LMOGs (fibers in spherulites) and CW being not a pure compound but comprising several n -alkanes besides hentriacontane.^{11,12}

In conclusion, these results obtained demonstrate that independent of the hydrogen bonding and dipolar interaction provided by the amide and the hydroxyl groups, the increase in the hydrocarbon chain length results in an increase in both the organogel resistance to deformation and its instant recovery capacity. However, the extended recovery capacity of the gel decreases. For units of similar length (i.e., HOA and O-HOA), the stabilization of the self-assembly unit through polar groups (i.e., $-\text{CONH}_2$ in HOA) reduces organogel elasticity but provides a higher extended recovery capacity, i.e., $\%R_{t=60\text{s}}$ and $\%R_{t=300\text{s}}$.

Organogelation using vegetable oils as the liquid phase is a promising alternative to modify the physical properties of vegetable oils without the use of chemical process that results in the formation of *trans*-fatty acids. The organogels developed by the LMOG amides investigated here have promising rheological properties for applications by the food industry. Among these is thixotropy, a desirable

attribute of many oil-based food systems such as vegetable spreads, edible coatings, chocolate spreads, and dressings. However, to the authors' knowledge, the amides investigated are not approved by the FDA for food use.

Fatty acid amides are found in nature, but are seldom encountered in significant quantity in edible fats and oils.¹⁷ However, they are produced on a large scale and used in the production of fiber lubricants, detergents, flotation agents, textile softeners, antistatic agents, mold release agents, and plasticizers for the polymer industry. On the other hand, recent studies have shown that some fatty acid amides, such as anandamide (i.e., *N*-arachidonylethanolamide)¹⁸ and oleamide (*cis*-9,10-octadecenamide),¹⁹ have specific biological functions. Arandamide has been shown to have anti-inflammatory and anti-cancer properties,¹⁸ and oleamide has been identified as the signaling molecule responsible for causing sleep.¹⁹

The results here reported showed some relationships between gelator structure and the thermo-mechanical properties of LMOG amides. Our long-term objective is to understand the organogelation process to eventually develop *trans*-free vegetable oil-based food products with novel textures for the consumers.

Acknowledgments The investigation was supported by grant no. 25706 from CONACYT. The technical support from Concepcion Maza-Moheno and Elizabeth Garcia-Leos is greatly appreciated. V. Ajay Mallia and Richard G. Weiss thank the U.S. National Science Foundation for its support of the research performed at Georgetown.

References

1. D.J. Abdallah, R.G. Weiss, *n*-Alkanes gel *n*-alkanes (and many other organic liquids). *Langmuir*. **16**, 352–355 (2000). doi:10.1021/1a990795r
2. E. Ostuni, P. Kamaras, R.G. Weiss, Novel X-ray method for in situ determination of gelator strand structure: polymorphism of cholesteryl anthraquinone-2-carboxylate. *Angew. Chem. Int. Ed Engl.* **35**, 1324–1326 (1996). doi:10.1002/anie.199613241
3. A. Bot, G.M. Agterof, Structuring of edible oils by mixtures of γ -oryzanol with β -sitosterol or related phytosterols. *J. Am. Oil Chem. Soc.* **83**, 513–521 (2006). doi:10.1007/s11746-006-1234-7
4. R. Kumar, O.P. Katare, Lecithin organogels as a potential phospholipid-structured system for topical drug delivery: a review. *AAPS PharmSciTech.* **6**, E298–E310 (2005). doi:10.1208/pt060240
5. S. Murdan, G. Gregoriadis, A.T. Florence, Novel sorbitan monostearate organogels. *J. Phar. Sci.* **88**, 608–614 (2000). doi:10.1021/js980342r
6. D.J. Abdallah, L. Lu, R.G. Weiss, Thermoreversible organogels from alkane gelators with one heteroatom. *Chem. Mater.* **11**, 2907–2911 (1999). doi:10.1021/cm9902826
7. H. Takeno, T. Mochizuki, K. Yoshida, S. Kondo, T. Dobashi, Self-assembling structures and sol-gel transition of optically active and racemic 12-hydroxystearic acids in organic solvents. *Progr. Colloid. Polym. Sci.* **136**, 47–54 (2009). doi:10.1007/2882_2009_7

8. V.A. Mallia, M. George, D.L. Blair, R.G. Weiss, Robust organogels from nitrogen-containing derivatives of (*R*)-12-hydroxystearic acid as gelators: comparisons with gels from stearic acid derivatives. *Langmuir*. **25**, 8615–8625 (2009). doi:[10.1021/la8042439](https://doi.org/10.1021/la8042439)
9. P. Terech, R.G. Weiss, Low molecular mass gelators of organic liquids and the properties of their gels. *Chem. Rev.* **97**, 3133–3159 (1997). doi:[10.1021/cr9700282](https://doi.org/10.1021/cr9700282)
10. R.G. Weiss, P. Terech, *Molecular Gels: Materials with Self-Assembled Fibrillar Networks* (Springer, Dordrecht, 2006), pp. 449–551
11. J.F. Toro-Vazquez, J.A. Morales-Rueda, E. Dibildox-Alvarado, M. A. Charó-Alonso, M. Alonzo-Macías, M.M. González-Chávez, Development of organogels with candelilla wax and safflower oil with high triolein content. *J. Am. Oil Chem. Soc.* **84**, 989–1000 (2007). doi:[10.1007/s11746-007-1139-0](https://doi.org/10.1007/s11746-007-1139-0)
12. J.A. Morales-Rueda, E. Dibildox-Alvarado, M. Charó-Alonso, R. G. Weiss, J.F. Toro-Vazquez, Thermo-mechanical properties of candelilla wax and dotriacontane organogels in safflower oil. *Europ. J. Lipid. Sci. Technol.* **111**, 207–215 (2009). doi:[10.1002/ejlt.200810174](https://doi.org/10.1002/ejlt.200810174)
13. J.A. Morales-Rueda, E. Dibildox-Alvarado, M.A. Charó-Alonso, J.F. Toro-Vazquez, Rheological properties of candelilla wax and dotriacontane organogels measured with a true-gap system. *J. Am. Oil Chem. Soc.* **86**, 765–772 (2009). doi:[10.1007/s11746-009-1414-3](https://doi.org/10.1007/s11746-009-1414-3)
14. M. Dolz, M.J. Hernández, J. Delegido, Creep and recovery experimental investigation of low oil content food emulsions. *Food Hydrocolloids*. **22**, 421–427 (2008). doi:[10.1016/j.foodhyd.2006.12.011](https://doi.org/10.1016/j.foodhyd.2006.12.011)
15. D.J. Abdallah, S.A. Sirchio, R.G. Weiss, Hexatriacontane organogels. The first determination of the conformation and molecular packing of a low-molecular-mass organogelator in its gelled state. *Langmuir*. **16**, 7558–7561 (2000). doi:[10.1021/la000730k](https://doi.org/10.1021/la000730k)
16. J.F. Steffe, *Rheological Methods in Food Process Engineering*, 2nd edn. (Freeman, East Lansing, 1996), pp. 304–310
17. The AOCS Lipid Library. Anandamide, oleamide and other simple fatty amides structure, occurrence, biology and analysis. <http://lipidlibrary.aocs.org/Lipids/amides/index.htm>
18. J. Joseph, B. Niggemann, K.S. Zaenker, F. Entschladen, Anandamide is an endogenous inhibitor for the migration of tumor cells and T lymphocytes. *Cancer Immunol. Immunother.* **53**, 723–728 (2004). doi:[10.1007/s00262-004-0509-9](https://doi.org/10.1007/s00262-004-0509-9)
19. S. Huitrón-Reséndiz, L. Gombart, B.F. Cravatt, S.J. Henriksen, Effect of oleamide on sleep and its relationship to blood pressure, body temperature, and locomotor activity in rats. *Exp. Neurol.* **72**, 235–243 (2001). doi:[10.1006/exnr.2001.7792](https://doi.org/10.1006/exnr.2001.7792)